AGU PUBLICATIONS

Water Resources Research

RESEARCH ARTICLE
10.1002/2015WR017990

Analytical solution and computer program (*FAST*) to estimate fluid fluxes from subsurface temperature profiles

Barret L. Kurylyk[1] and Dylan J. Irvine[2,3]

[1]Department of Geoscience, University of Calgary, Calgary, Alberta, Canada, [2]School of Earth, Atmosphere and Environment, Monash University, Clayton, Victoria, Australia, [3]National Centre for Groundwater Research and Training, Flinders University, Adelaide, South Australia, Australia

Key Points:
- A solution is derived to estimate subsurface water flow from temperature
- The boundary and initial conditions are more flexible than in past solutions
- A new program *FAST* is presented to facilitate solution inversion

Supporting Information:
- Supporting Information S1
- Software S1
- Software S2

Correspondence to:
D. J. Irvine,
dylan.irvine@monash.edu

Citation:
Kurylyk, B. L., and D. J. Irvine (2016), Analytical solution and computer program (*FAST*) to estimate fluid fluxes from subsurface temperature profiles, *Water Resour. Res.*, *52*, 725–733, doi:10.1002/2015WR017990.

Received 20 AUG 2015
Accepted 13 JAN 2016
Accepted article online 18 JAN 2016
Published online 5 FEB 2016

Abstract This study details the derivation and application of a new analytical solution to the one-dimensional, transient conduction-advection equation that is applied to trace vertical subsurface fluid fluxes. The solution employs a flexible initial condition that allows for nonlinear temperature-depth profiles, providing a key improvement over most previous solutions. The boundary condition is composed of any number of superimposed step changes in surface temperature, and thus it accommodates intermittent warming and cooling periods due to long-term changes in climate or land cover. The solution is verified using an established numerical model of coupled groundwater flow and heat transport. A new computer program *FAST* (Flexible Analytical Solution using Temperature) is also presented to facilitate the inversion of this analytical solution to estimate vertical groundwater flow. The program requires surface temperature history (which can be estimated from historic climate data), subsurface thermal properties, a present-day temperature-depth profile, and reasonable initial conditions. *FAST* is written in the Python computing language and can be run using a free graphical user interface. Herein, we demonstrate the utility of the analytical solution and *FAST* using measured subsurface temperature and climate data from the Sendia Plain, Japan. Results from these illustrative examples highlight the influence of the chosen initial and boundary conditions on estimated vertical flow rates.

1. Introduction

Subsurface thermal regimes are perturbed by mobile groundwater, and thus temperature can be used as an environmental tracer to determine the direction and magnitude of groundwater flow [*Anderson*, 2005]. Several studies [e.g., *Hatch et al.*, 2006; *Keery et al.*, 2007; *Luce et al.*, 2013] have recently developed processes to estimate rates of groundwater-surface interactions from daily temperature signals at different depths. These and other techniques have been automated in computer programs including Ex-Stream [*Swanson and Cardenas*, 2011], VFLUX [*Gordon et al.*, 2012; *Irvine et al.*, 2015], 1DTempPro [*Voytek et al.*, 2014], and LPML [*Vandersteen et al.*, 2015].

Tracing groundwater flow via the propagation of daily or seasonal surface temperature signals is restricted to shallow subsurface environments as these high-frequency signals are fully attenuated in the deeper subsurface. However, deep subsurface temperature profiles can also be analyzed to infer rates of groundwater flow using other techniques. *Bredehoeft and Papadopulos* [1965] derived a solution to the one-dimensional, steady state, conduction-advection equation that could be applied to estimate groundwater flow rates from the curvature of temperature-depth (*T-z*) profiles. Other steady state solutions were subsequently developed to accommodate more complex environments [*Lu and Ge*, 1996; *Mansure and Reiter*, 1979] and these are included in the "heatfuncs" library for the Python programming language [*Irvine*, 2015]. However, these steady state approaches do not account for the transient subsurface thermal effects of past climate change or land cover disturbances [*Kurylyk et al.*, 2015]. Because groundwater flow and climate change can both disturb subsurface thermal regimes, the mechanism for causing thermal anomalies (e.g., deviations from the geothermal gradient) can arise from either process [*Ferguson et al.*, 2006; *Ferguson and Woodbury*, 2005; *Kukkonen et al.*, 1994; *Majorowicz et al.*, 2006]. Thus, solutions to the transient conduction-advection equation have been proposed that accommodate a sudden step change in surface temperature [*Taniguchi et al.*, 1999a] or a smooth gradually increasing surface temperature function [*Kurylyk and MacQuarrie*, 2014; *Taniguchi et al.*, 1999b]. Surface temperature trends violate these idealized boundary conditions (i.e., smooth

persistent trends or a single step change) due to intermittent warming and cooling periods caused by the interplay between factors such as anthropogenic forcing, episodic volcanic activity, and multidecadal oceanic oscillations [*Intergovernmental Panel on Climate Change*, 2013].

Menberg et al. [2014] demonstrated that superposition principles could be applied to allow for a series of step increases in temperature and thus accommodate the influence of several climate regime shifts. However, the application of the *Menberg et al*. [2014] solution is limited to the shallow subsurface as uniform initial temperature conditions (i.e., no geothermal gradient) are assumed. Thus, the utility of previous analytical solutions for tracing groundwater flow from subsurface temperature profiles has been limited by the lack of realism in the surface temperature boundary condition and/or initial conditions.

An improved approach that allows for both flexible boundary and initial conditions will allow for more robust vertical groundwater flux/recharge estimation, which is recognized as an important component of effective water management [*Scanlon et al*., 2006; *Scanlon and Cooke*, 2002]. The objectives of the present study are threefold:

1. Derive a new analytical solution with flexible initial conditions and a boundary condition that accommodates intermittent surficial warming and cooling periods.
2. Present a computer program that facilitates the inversion of this solution to infer flow rates from *T-z* profiles.
3. Demonstrate the application of the program using measured subsurface temperature data.

The previously proposed analytical solutions and the new solution presented in this study can be challenging to implement, and thus the computer program is developed to facilitate the utility of the new solution. For example, the solution presented here can be applied through the use of spreadsheet software; however, this approach can be extremely cumbersome, particularly if multiple changes to the boundary condition are required. In contrast, changes to initial or boundary conditions can be easily handled through automated computer software. The utility of the new program is demonstrated by analyzing subsurface temperature data collected for a well in the Sendai Plain, Japan [*Gunawardhana et al*., 2011].

Analytical solutions for tracing groundwater flow from subsurface temperature offer potential advantages over numerical methods including: increased efficiency for poorly defined systems, increased stability and independence from spatiotemporal discretization, and limited degrees of freedom to facilitate analyses of interactions between parameters and solutions [*Kurylyk and MacQuarrie*, 2014; *Javandel et al*., 1984].

2. Methods

2.1. Theory and Derivation of Analytical Solution

The governing equation for one-dimensional subsurface heat transport in a homogeneous medium with constant groundwater velocity can be written as [*Carslaw and Jaeger*, 1959]

$$D\frac{\partial^2 T}{\partial z^2} - v_t\frac{\partial T}{\partial z} = \frac{\partial T}{\partial t} \tag{1}$$

where T is temperature (°C), z is depth (m, positive downward), t is time (s), D is the bulk thermal diffusivity ($m^2\ s^{-1}$), and v_t is the thermal plume velocity due to advection ($m\ s^{-1}$, positive downward). Note that v_t is related to the Darcy flux [e.g., *Hatch et al*., 2006]

$$v_t = q\frac{c_w\rho_w}{c\rho} \tag{2}$$

where q is the Darcy flux ($m\ s^{-1}$), $c_w\rho_w$ is the volumetric heat capacity of water ($J\ m^{-3}°C^{-1}$), and $c\rho$ is the bulk volumetric heat capacity of the saturated medium ($J\ m^{-3}°C^{-1}$). Thus, the Darcy flux can be obtained if v_t is known. The terms in equations (1) and (2) are provided in standard SI units; however, it is often more convenient to work with years as the standard time unit when dealing with long-term changes, and thus D, t, v_t, and q can be expressed in units of $m^2\ yr^{-1}$, yr, $m\ yr^{-1}$, and $m\ yr^{-1}$, respectively. Herein, we ignore the effects of thermal dispersion, which are normally insignificant for slow vertical groundwater flow due to the efficiency of heat diffusion [*Bear*, 1972]. More details concerning terms in equation (1) can be found in *Kurylyk et al*. [2014]. Assumptions invoked by equation (1) are discussed later.

Most previous solutions to equation (1) assume a constant or linear initial *T-z* profile; however, the initial condition function can be better represented using a combination of linear and exponential functions:

$$\text{Initial condition}: T(z,t=0)=T_i+a\,z+\delta\exp(dz) \tag{3}$$

where $T_i+\delta$ is the initial temperature at the land surface (°C), a is the general geothermal gradient (°C m^{-1}), and d (m^{-1}) is a fitting parameter to account for curvature in the *T-z* profile due to past climate change, land cover disturbances, or vertical groundwater flow. Examples of the ability of this function to match present-day *T-z* profiles beneath the Sendai Plain and Tokyo, Japan, are provided by *Kurylyk and MacQuarrie* [2014].

The original surface temperature step function presented by *Taniguchi et al*. [1999a] to account for land cover changes can be superimposed to represent a series of sequential step changes in surface temperature due to climate change or land cover alterations:

$$\text{Boundary condition}: T(z=0,t)=T_0+\sum_{j=1}^{n}\Delta T_j\times H(t-t_j) \tag{4}$$

where T_0 is the initial surface temperature ($=T_i+\delta$, °C), ΔT_j is the jth surface temperature shift (°C), t_j represents the timing of shift j (s or year depending on fundamental time unit), and H is the Heaviside function which indicates that the influence of each shift is not realized until the time t exceeds t_j (i.e., $H(t\text{-}t_j)=0$ before t_j and 1 after t_j). The magnitudes of each shift (ΔT_j) are evaluated as the difference in the surface temperature before and after shift j.

The governing partial differential equation (equation (1)) is reduced to an ordinary differential equation via the Laplace transform technique and the initial condition. The resultant ordinary differential equation in the frequency domain is solved using the surface boundary condition (equation (4)) and assuming a semi-infinite domain. The resultant solution is then converted back into the time domain via inverse Laplace transforms. More details are provided in Text S1 of Supporting Information S1. The final solution is presented in equation (5).

$$\begin{aligned}T={}&az+T_i-v_t at+\delta\exp(Dd^2t+dz-v_t dt)\\&+\sum_{j=1}^{n}\left\{\frac{\Delta T_j}{2}\left[\operatorname{erfc}\left(\frac{z-v_t(t-t_j)}{2\sqrt{D(t-t_j)}}\right)+\exp\left(\frac{v_t z}{D}\right)\operatorname{erfc}\left(\frac{z+v_t(t-t_j)}{2\sqrt{D(t-t_j)}}\right)\right]H(t-t_j)\right\}+\\&\frac{T_0-T_i}{2}\left[\operatorname{erfc}\left(\frac{z-v_t t}{2\sqrt{Dt}}\right)+\exp\left(\frac{v_t z}{D}\right)\operatorname{erfc}\left(\frac{z+v_t t}{2\sqrt{Dt}}\right)\right]+\frac{a}{2}\left\{(v_t t-z)\operatorname{erfc}\left(\frac{z-v_t t}{2\sqrt{Dt}}\right)+(v_t t+z)\exp\left(\frac{v_t z}{D}\right)\operatorname{erfc}\left(\frac{z+v_t t}{2\sqrt{Dt}}\right)\right\}-\\&\frac{\delta}{2}\exp\left\{\frac{v_t z}{2D}+Dd^2t-v_t dt\right\}\left\{\begin{array}{l}\exp\left(-z\sqrt{{v_t^2}/{4D^2}+d^2-{v_t d}/{D}}\right)\operatorname{erfc}\left(\dfrac{z}{2\sqrt{Dt}}-\sqrt{\dfrac{v_t^2 t}{4D}+Dd^2t-v_t dt}\right)\\+\exp\left(z\sqrt{{v_t^2}/{4D^2}+d^2-{v_t d}/{D}}\right)\operatorname{erfc}\left(\dfrac{z}{2\sqrt{Dt}}+\sqrt{\dfrac{v_t^2 t}{4D}+Dd^2t-v_t dt}\right)\end{array}\right\}\end{aligned} \tag{5}$$

Practical suggestions for parameterizing the boundary and initial condition functions and applying equation (5) are provided in Text S2 of Supporting Information S1. This solution is verified using the finite element groundwater and heat transport model SUTRA [*Voss and Provost*, 2010]. Details regarding the solution verification are provided in Text S3 in Supporting Information S1.

2.2. *FAST* Computer Program

The *FAST* (Flexible Analytical Solution based on Temperature) functions (for equations (3)–(5)) are written in the Python programming language (version 2.7 or later). The *FAST.py* script (Software S1) must be run once to compile the script and make the functions available for use.

The process of running *FAST* is a three-step process (Figure 1) that provides the maximum flexibility for exploring options for both the boundary conditions (using *FASTbc*, i.e., equation (4)) and initial conditions (using *FASTic*, i.e., equation (3)) of the problem, before the outputs from equations (3) and (4) are

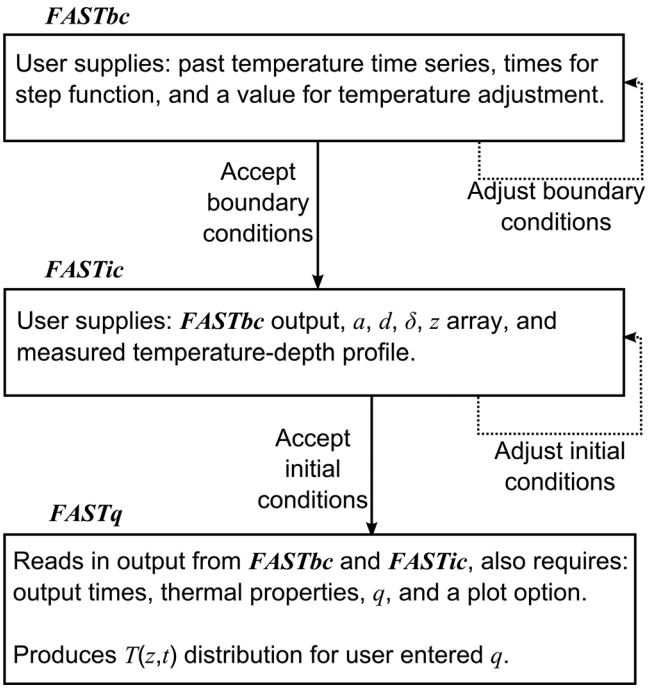

Figure 1. Work flow for the *FAST* functions. The *FASTbc* and *FASTic* functions produce the boundary and initial conditions for the *FASTq* function.

used to calculate $T(z,t)$ via equation (5). It is important to note that the *FAST* functions must be run in the following order: *FASTbc*, *FASTic*, and *FASTq* (Figure 1). Once *FAST.py* has been run (compiled), a separate short script (see example in supporting information Software S2) can be employed to read in the specific thermal properties and boundary and initial condition data from text files.

In addition to the descriptions of the individual functions below, plotting options are coded into the *FASTbc* and *FASTic* functions. These options can be altered by making changes in the *FAST.py* file, and recompiling (rerunning) the *FAST.py* script. Guidance on using *FAST*, making appropriate code changes, installation of Python, and basic Python programming resources are provided in the detailed *FAST* manual provided in Text S4 of Supporting Information S1.

2.2.1. Prepare Boundary Conditions (FASTbc)

FASTbc requires a time series of past temperature (time and temperature) to be entered as individual arrays with units of year and °C, respectively. These data may be estimated from regional or local historical climate (surface air temperature) data or obtained directly from measurements of ground surface temperatures or surface temperature modeling. *FASTbc* also requires an array of times (i.e., t_j, in equation (4), denoted as *ttimes* in the code, see Text S4 of Supporting Information S1) that are used for the calculation of the step function of temperature (i.e., ΔT_j). Essentially, *FASTbc* calculates the average surface temperature for each interval between *ttimes* values and then evaluates each ΔT_j as the difference in the average surface temperatures for intervals j and $j-1$.There is no requirement for these times to be evenly spaced.

Additionally, a constant offset (T_{adj}) can be applied to adjust all of the temperature values in the outputted temperature array if air, rather than surface, temperature were used to populate the temperature array. T_{adj} is included in *FASTbc* to take into account snowpack or forest canopy insulation or other processes that may cause an offset between mean annual air and ground surface temperatures [*Zhang*, 2005].

An example output of the *FASTbc* function for climate data from Mount Barker in South Australia for time intervals of varying length is shown in Figure 2. *FASTbc* calculates T_0 as the mean temperature between the start of the user provided temperature time series, and the time of the first value of *ttimes* (i.e., black line from 1927 to 1942, Figure 2).

2.2.2. Prepare Initial Conditions (FASTic)

The *FASTic* function reads in (1) output from the *FASTbc* function, (2) values for a, d, δ, (3) an array of depths (z) for the initial and final $T(z,t)$ output, and (4) a field measured T-z profile (see sample file for reading in data provided in supporting information Software S2). The T_0 value from the *FASTbc* function and the user provided δ value are used to calculate T_i (used in equations (3) and (5)), hence *FASTbc* must be run prior to *FASTic*. The field measured T-z profile is not involved in any calculations in *FASTic*, but rather is plotted along with the output of *FASTic* (equation (3)) to provide a visual comparison between the field data and the imposed initial conditions.

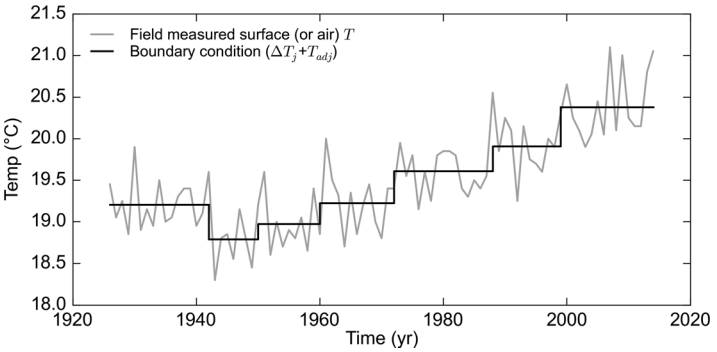

Figure 2. Example output from *FASTbc* for air temperature data from Mount Barker in South Australia (gray), data available at: http://www.bom.gov.au/climate/data/. The boundary condition $T_j + T_{adj}$ is shown for *ttimes* = [1942, 1950, 1960, 1972, 1988, 1999], using, $T_{adj} = 0$ °C.

2.2.3. Running the Solution (FASTq)

The final step is to run the *FASTq* function, in which values of *T*(*z*,*t*) are calculated with equation (5). In addition to the output from the *FASTbc* and *FASTic* functions, the user must also provide output times (i.e., *outtimes*) for the analytical solution, thermal properties of the system, a value for *q* (m yr^{-1}) and a value for the plotoption (0 = no plot, 1 = plot shown to screen).

FASTq calculates the bulk thermal diffusivity (*D*, m^2 s^{-1}) using the volumetrically weighted geometric mean of water and sediment thermal conductivities to obtain the bulk thermal conductivity (λ) and volumetrically weighted arithmetic mean of the water and sediment volumetric heat capacities to obtain the bulk volumetric heat capacity ($c\rho$) [*Lunardini*, 1981]. All inputs for thermal properties must use J, W, kg, m, and °C.

The result from the *FASTq* function is the *T*(*z*,*t*) distribution for the user provided properties (boundary conditions, initial conditions, thermal properties, and *q*) and times. The flexibility of the *FASTbc*, *FASTic*, and *FASTq* functions allows for the investigation of the influence of the initial conditions, boundary conditions, thermal properties, or *q* on the resulting *T*(*z*,*t*). The user can vary these inputs in order to best match *T*(*z*,t_n) with the field measured *T*-*z* profile. The sum of squared errors (SSE) and the RMSE between the observed *T*-*z* profile and the final *T*(*z*,t_n) are outputted to provide guidance on how well the solution has reproduced the observed *T*-*z* profile. We acknowledge that the flexibility of the boundary and initial conditions introduces additional uncertainty not encountered in previous, simpler solutions. However, previous approaches overlooked these sources of uncertainty by employing potentially overly simplistic techniques. In *FAST*, these uncertainties can be explicitly accounted for by testing the influence of these properties on the inverted Darcy flux.

3. Field Application of *FAST*

3.1. Site Conditions and *FAST* Thermal Property Inputs

We herein provide two illustrative *FAST* examples by estimating vertical water flow using local surface air temperature history and a temperature profile collected from a well in the Sendai Plain, Japan ("Well 1") [*Gunawardhana et al*., 2011]. Vertical heat transfer and groundwater flow in the Sendai Plain is much higher than horizontal heat transfer and groundwater flow [*Gunawardhana et al*., 2011], and thus the one-dimensional assumption of the solution is justified. The porosity, λ, and $c\rho$ for this region were, respectively, chosen to be 0.2, 1.4 W m^{-1} °C^{-1}, and 2.325 × 10^6 J m^{-3} °C^{-1} following *Uchida and Hayashi* [2005]. These properties can be used to indirectly obtain estimates for the other *FAST* thermal property inputs, namely the thermal conductivity of the solid grains (1.65 W m^{-1} °C^{-1}) and the volumetric heat capacity of the solid grains (1.86 × 10^6 J m^{-3} °C^{-1}), by using standard values of 4.18 × 10^6 J m^{-3} °C^{-1} and 0.6 W m^{-1} °C^{-1} for water heat capacity and thermal conductivity, respectively, and by rearranging the bulk thermal property equations (see Text S4 of Supporting Information S1).

3.2. Boundary Conditions for *FAST* Examples

The surface temperatures for these illustrative examples are estimated from the nearby long-term climate station in the Sendai Plain [*Japanese Meteorological Agency*, 2015]. Although pronounced air temperature warming is evident in the latter half of the 1900s, climate data prior to 1950 were relatively stable in this region. The subsurface temperature profile (Figure 3a) was measured in 2008 [*Gunawardhana et al*., 2011]. Hence, in this study, only air temperature data between 1940 (*t* = 0, equation (5)) and 2007 (*t* = 67 years) are considered, with the 1940–1949 air temperature used to determine the initial conditions in *FASTbc*.

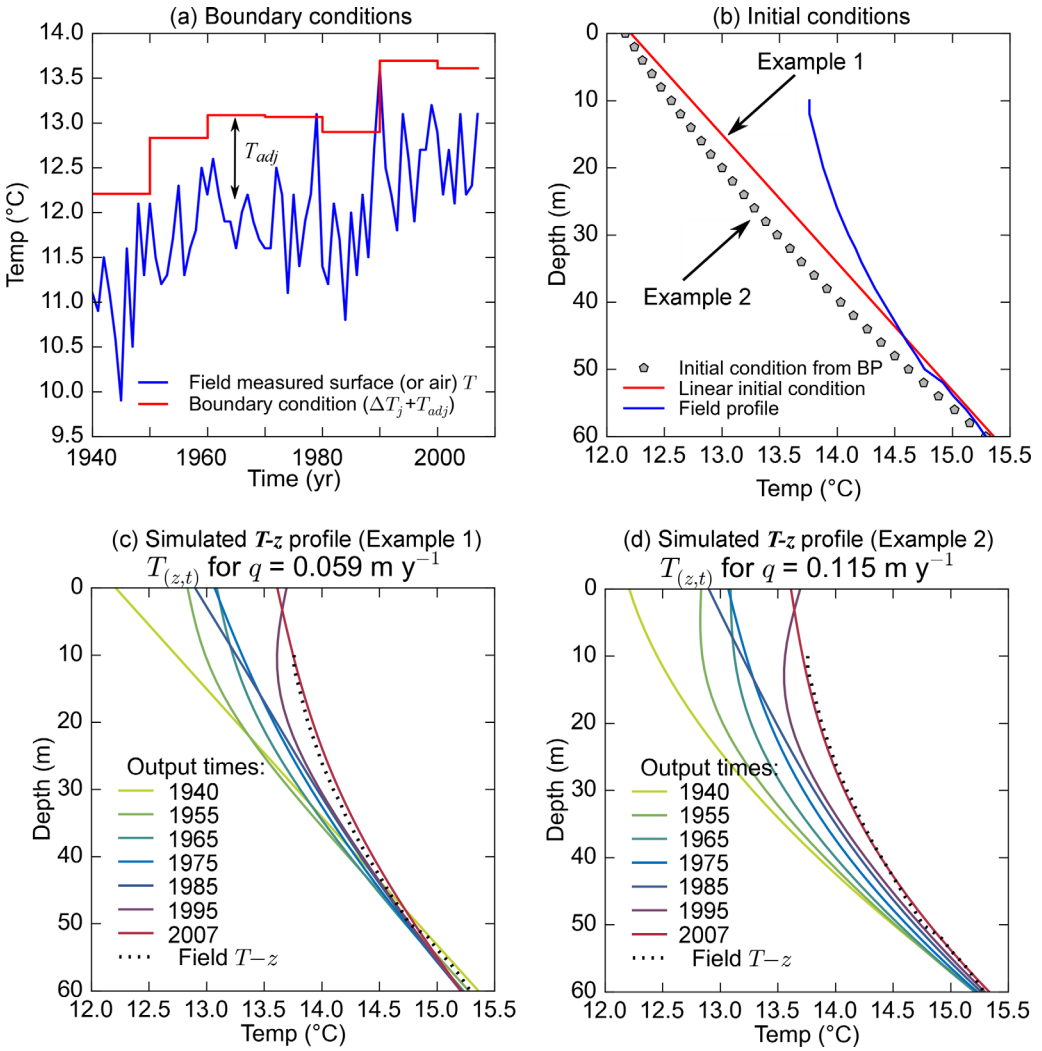

Figure 3. (a) Surface air temperature data and boundary condition from *FASTbc* (Section 3.2). (b) Initial conditions assuming a linear profile (Example 1) or a non-linear profile (Example 2) based on the Bredehoeft and Papadopulos [1965] solution (Section 3.2). Eq. (3) parameters are provided in the text. (c) *FASTq* results for Example 1 in (b) (Section 3.4). (d) *FASTq* results for Example 2 in (b) (Section 4). Vertical flow rates are indicated in the titles for (c) and (d).

Figure 3a presents these climate data (plus T_{adj}) averaged out in *FASTbc* for 10 year time intervals between 1940 and 2000 (i.e., 1940s, 1950s, and so forth) and for 7 years from 2001 to 2007.

FASTbc calculates the initial surface temperature from the average of the boundary temperature in the first interval (11.06 °C for 1940–1949, Figure 3a) plus potentially some thermal offset (T_{adj}) to account for the difference in mean annual air and surface temperatures. As described in detail in Text S2 of Supporting Information S1, one option for determining the desired initial conditions is to extrapolate the deeper, undisturbed geothermal (i.e., linear) gradient to the surface (Example 1, Figure 3b). This extrapolation process, which is herein used to obtain a value for T_{adj}, yields a surface temperature of 12.16 °C. For this example, T_{adj} is estimated as the difference between the geothermal gradient extrapolated to the ground surface and the mean annual air temperature from 1940 to 1949 (T_{adj} = 12.16 °C − 11.06 °C = 1.1 °C). This thermal offset is reasonable as the meteorological station is located on the perimeter of the city, whereas the well in which the temperature profile was recorded is located closer to the city center and would thus experience slightly warmer surface and subsurface conditions (L.N. Gunawardhana, personal communication, 2015).

3.3. Initial Conditions for *FAST* Examples

The shallow portion of the *T-z* profile (Figure 3b) has been influenced by the post-1950 warming presented in Figure 3a, but the deeper profile appears to be unperturbed by recent surface temperature change. As

noted above, the initial conditions for the first example are chosen by extrapolating the undisturbed linear portion of the *T-z* profile (50–60 m) to the land surface. This profile yields initial condition (equation (3)) parameters T_i, a, δ, and d of 12.16 °C, 0.0525 °C m^{-1}, 0 °C, and 0 m^{-1}, respectively (Figure 3b). This profile is denoted as "Example 1" in Figure 3b.

A second example (Example 2, Figure 3b) is also provided to demonstrate how the solution can accommodate nonlinear initial conditions and to investigate how these conditions may influence the estimation of the vertical flow rate. The second initial condition is found by first calculating the steady state profile using the *Bredehoeft and Papadopulos* [1965] solution with the upper fixed temperature, lower fixed temperature, and q chosen as 12.16 °C, 15.29 °C, and 0.105 m yr^{-1}. The lower temperature was taken as the measured temperature at a depth of 60 m, the upper temperature was chosen based on the climate data and T_{adj} (section 3.2), and the vertical flow rate was obtained from *Gunawardhana et al*. [2011, Table 3].

In theory, the *Bredehoeft and Papadopulos* [1965] solution should provide the 1940 temperature profile for uniform vertical flow and the stable Sendai Plain climate preceding this period. The curvature of this particular profile is not high given the low vertical flow in this well compared to nearby wells [*Gunawardhana et al*., 2011, Table 3]. The steady state profile from the *Bredehoeft and Papadopulos* [1965] solution must be matched with the initial condition function (equation (3)) to be applied as initial conditions. The nonlinear initial *T-z* profile for this example ("Example 2," Figure 3b) was generated by setting T_i, a, δ, and d to −1.53 °C, 0.152 °C m^{-1}, 13.74 °C, and −0.00976 m^{-1}, respectively (equation (3)). These initial condition parameters yield an RMSE of only 0.02 °C when compared to the results obtained from the *Bredehoeft and Papadopulos* [1965] solution.

3.4. Results From the Illustrative Examples

FASTq was run using the boundary condition obtained from *FASTbc* (Figure 3a) and the initial conditions generated in *FASTic* (Figure 3b). For the initial conditions obtained by extrapolating the geothermal gradient to the land surface (Example 1, *FASTic*), a reasonable fit (RMSE = 0.047 °C) between the measured *T-z* profile and the final calculated *T-z* profile was found using a downward Darcy flux of 0.059 m yr^{-1} (Figure 3c). It is important to note that this is approximately half of the Darcy flux (0.105 m yr^{-1}) estimated by *Gunawardhana et al*. [2011] using the approach of *Taniguchi et al*. [1999b] for this particular well. This difference highlights the potential influence of the boundary condition choice (i.e., step function versus linear trend).

The *FASTq* results for the second initial condition example are presented in Figure 3d. Due to the curvature of the chosen initial conditions, higher Darcy fluxes are required to match the present-day *T-z* profile. A good fit (RMSE = 0.025 °C, Figure 3d) was obtained using a Darcy flux of 0.115 m yr^{-1}, which is close to the value (0.105 m yr^{-1}) assumed for the initial conditions. The considerable difference in the estimated fluxes for the two initial conditions (Figure 3c versus Figure 3d) illustrates the influence of the initial conditions and thus demonstrates the potential errors introduced by assuming a linear initial *T-z* profile. This field example is intended to demonstrate the utility of *FAST*; more practical discussions for parameterizing and applying *FAST* are provided in Text S2 of Supporting Information S1.

4. Limitations

There are several limitations associated with the governing heat transfer equation (equation (1)). Most notably this equation assumes that the heat transfer is constrained to the vertical direction. This assumption may be violated in subsurface environments where there are strong lateral thermal gradients or in aquifers with lateral groundwater flow [*Ferguson and Beltrami*, 2006]. The governing equation also assumes that the thermal diffusivity and thermal plume velocity due to advection are steady and uniform. Heterogeneities in thermal properties due to soil layering frequently occur in subsurface profiles and can influence subsurface thermal regimes [*Ferguson*, 2007]. However, it should be noted that the variability in thermal properties is typically orders of magnitude less than the variability in hydraulic properties [e.g., *Anderson*, 2005]. Vertical water flow rates may change with time and space due to the vertical distribution of hydraulic properties and precipitation changes arising from climate change. Finally, this equation assumes that no pore water phase change occurs, and thus the method should not be employed in permafrost environments, at least where soil freeze-thaw occurs. Despite these assumptions, the equation

proposed in this study represents an improvement to existing analytical solutions that are applied for tracing groundwater flow from *T-z* profiles due to the enhanced flexibility in both the boundary and initial conditions.

5. Conclusion and Future Directions

This study has presented a new analytical solution to the one-dimensional, transient conduction-advection equation. The flexibility in the initial and boundary conditions allows users to match subsurface and atmospheric conditions more closely and thus enhances fidelity to physical processes.

One difficulty associated with the new solution is that it cannot be readily incorporated into spreadsheet software due to the complex nature of the boundary condition (i.e., the superimposed surface temperature shifts). To overcome this limitation, this study has also presented an open access software program, *FAST*, to facilitate the application of this solution using long-term climate data. This program also enables users to efficiently conduct sensitivity analyses by varying the input parameters and evaluating the resultant influence on *T-z* profiles or the Darcy flux.

We have predominantly focused on the utility of the analytical solution to estimate groundwater flow rates from present-day *T-z* profiles and knowledge of surface temperature history. However, the solution could also applied in a forward manner to estimate the influence of future climate change or land cover disturbances on present-day groundwater temperature in the same manner that other, more restrictive, solutions have been applied [*Gunawardhana and Kazama*, 2011; *Gunawardhana et al*., 2011; *Kurylyk and MacQuarrie*, 2014; *Kurylyk et al*., 2015]. Another potential application of this solution and *FAST* is paleoclimate inversion. Previous paleoclimate inversions from borehole temperature profiles have generally relied on solutions to the heat diffusion equation [*Harris and Chapman*, 1997; *Mareschal and Beltrami*, 1992], and this new solution, which accommodates advection, may provide an alternative for boreholes with known vertical flow rates. Finally, the solution may also be applied to estimate rates of groundwater-surface interactions and thus provide an improvement on existing temperature-based methods that require either periodic or steady boundary conditions [e.g., *Caissie et al*., 2014]. In this case, shallower temperature profiles would be analyzed, and the time intervals for obtaining the surface temperature step changes would be much shorter (e.g., hourly or daily) than in the present study. Future studies will investigate these alternative solution applications.

Acknowledgments
Data presented in this paper can be obtained by contacting either author. The *FAST* computer program and associated documentation are included in the supporting information. We thank Luminda Gunawardhana of Sultan Qaboos University for providing the temperature data beneath the Sendai Plain. B. Kurylyk and D. Irvine contributed equally to this work. Constructive comments from two anonymous peer reviewers, the Associate Editor, and the Editor Harihar Rajaram improved the quality of this manuscript. B. Kurylyk was funded via postdoctoral fellowships provided by the Natural Sciences and Engineering Research Council of Canada, the Killam Trusts, and the University of Calgary Eyes High program.

References

Anderson, M. P. (2005), Heat as a ground water tracer, *Ground Water*, *43*, 951–968, doi:10.1111/j.1745-6584.2005.00052.x.
Bear, J. (1972), *Dynamics of Fluids in Porous Media*, Elsevier, N. Y.
Bredehoeft, J. D., and I. S. Papadopulos (1965), Rates of vertical groundwater movement estimated from the Earth's thermal profile, *Water Resour. Res.*, *1*, 325–328, doi:10.1029/WR001i002p00325.
Caissie, D., B. L. Kurylyk, A. St-Hilaire, N. El-Jabi, and K. T. B. MacQuarrie (2014), Streambed temperature dynamics and corresponding heat fluxes in small streams experiencing seasonal ice cover, *J. Hydrol.*, *519*, 1441–1452, doi:10.1016/j.jhydrol.2014.09.034.
Carslaw, H. S., and J. C. Jaeger (1959), *Conduction of Heat in Solids*, Clarendon, Oxford, U. K.
Ferguson, G. (2007), Heterogeneity and thermal modeling of ground water, *Ground Water*, *45*, 485–490, doi:10.1111/j.1745-6584.2007.00323.x.
Ferguson, G., and H. Beltrami (2006), Transient lateral heat flow due to land-use changes, *Earth Planet. Sci. Lett.*, *242*, 217–222, doi:10.1016/j.epsl.2005.12.001.
Ferguson, G., and A. D. Woodbury (2005), The effects of climatic variability on estimates of recharge from temperature profiles, *Ground Water*, *43*(6), 837–842, doi:10.1111/j.1745-6584.2005.00088.x.
Ferguson, G., H. Beltrami, and A. D. Woodbury (2006), Perturbation of ground surface temperature reconstructions by groundwater flow?, *Geophys. Res. Lett.*, *33*, L13708, doi:10.1029/2006GL026634.
Gordon, R. P., L. K. Lautz, M. A. Briggs, and J. M. McKenzie (2012), Automated calculation of vertical pore-water flux from field temperature time series using the VFLUX method and computer program, *J. Hydrol.*, *420–421*, 142–158, doi:10.1016/j.jhydrol.2011.11.053.
Gunawardhana, L. N., and S. Kazama (2011), Climate change impacts on groundwater temperature change in the Sendai plain, Japan, *Hydrol. Processes*, *25*, 2665–2678, doi:10.1002/hyp.8008.
Gunawardhana, L. N., S. Kazama, and S. Kawagoe (2011), Impact of urbanization and climate change on aquifer thermal regimes, *Water Res. Manage.*, *25*, 3247–3276, doi:10.1007/s11269-011-9854-6.
Harris, R. N., and D. S. Chapman (1997), Borehole temperatures and a baseline for 20th-century global warming estimates, *Science*, *275*, 1618–1621, doi:10.1126/science.275.5306.1618.
Hatch, C. E., A. T. Fisher, J. S. Revenaugh, J. Constantz, and C. Ruehl (2006), Quantifying surface water-groundwater interactions using time series analysis of streambed thermal records: Method development, *Water Resour. Res.*, *42*, W10410, doi:10.1029/2005WR004787.
Intergovernmental Panel on Climate Change (2013), *Climate Change 2013: The Physical Science Basis. Contribution of Working Group I to the Fifth Assessment Report of the Intergovernmental Panel on Climate Change*, edited by T. F. Stocker et al., Cambridge Univ. Press, N. Y.

Irvine, D. J. (2015), How to use the heatfuncs Python library to calculate groundwater flow from temperature data, doi:10.13140/2.1.1632.5442. [Available at https://www.researchgate.net/publication/270884674_How_to_use_the_heatfuncs_Python_library_to_calculate_groundwater_flow_from_temperature_data?ev=prf_pub.]

Irvine, D. J., L. K. Lautz, M. A. Briggs, R. P. Gordon, and J. M. McKenzie (2015), Experimental evaluation of the applicability of phase, amplitude, and combined methods to determine water flux and thermal diffusivity from temperature time series using VFLUX 2, *J. Hydrol.*, *531*, 728–737, doi:10.1016/j.jhydrol.2015.10.054.

Japanese Meteorological Agency (2015), *Long Term Climate Data From the Sendai Plain*, Tokyo, Japan. [Available at http://www.data.jma.go.jp/obd/stats/etrn/index.php?prec_no=34&block_no=47590&year=2006&month=05&day=17&view=p1.]

Javandel, I., C. Doughty, and C. Tsang (1984), *Groundwater Transport: Handbook of Mathematical Models*, AGU, Washington, D. C.

Keery, J., A. Binley, N. Crook, and J. W. N. Smith (2007), Temporal and spatial variability of groundwater-surface water fluxes: Development and application of an analytical method using temperature time series, *J. Hydrol.*, *336*, 1–16, doi:10.1016/j.jhydrol.2006.12.003.

Kukkonen, I. T. T., V. Cermák, and J. Safanda (1994), Subsurface temperature-depth profiles, anomalies due to climatic ground surface temperature changes or groundwater flow effects, *Global Planet. Change*, *9*, 221–232, doi:10.1016/0921-8181[94]90017-5.

Kurylyk, B. L., and K. T. B. MacQuarrie (2014), A new analytical solution for assessing climate change impacts on subsurface temperature, *Hydrol. Processes*, *28*, 3161–3172, doi:10.1002/hyp.9861.

Kurylyk, B. L., K. T. B. MacQuarrie, and J. M. McKenzie (2014), Climate change impacts on groundwater and soil temperatures in cold and temperate regions: Implications, mathematical theory, and emerging simulation tools, *Earth Sci. Rev.*, *138*, 313–334, doi:10.1016/j.earscirev.2014.06.006.

Kurylyk, B. L., K. T. B. MacQuarrie, D. Caissie, and J. M. McKenzie (2015), Shallow groundwater thermal sensitivity to climate change and land cover disturbances: Derivation of analytical expressions and implications for stream temperature modeling, *Hydrol. Earth Syst. Sci.*, *19*, 2469–2489, doi:10.5194/hess-19-2469-2015.

Lu, N., and S. Ge (1996), Effect of horizontal heat and fluid flow on the vertical temperature distribution in a semiconfining layer, *Water Resour. Res.*, *32*, 1449–1453, doi:10.1029/95WR03095.

Luce, C. H., D. Tonina, F. P. Gariglio, and R. Applebee (2013), Solutions for the diurnally forced advection-diffusion equation to estimate bulk fluid velocity and diffusivity in streambeds from temperature time series, *Water Resour. Res.*, *49*, 488–506, doi:10.1029/2012WR012380.

Lunardini, V. J. (1981), *Heat Transfer in Cold Climates*, Van Nostrand Reinhold, N. Y.

Majorowicz, J. A., S. E. Grasby, G. Ferguson, J. Safanda, and W. Skinner (2006), Paleoclimatic reconstructions in western Canada from boreholetemperature logs: Surface air temperature forcing and groundwater flow, *Clim. Past*, *2*, 1–10, doi:10.5194/cp-2-1-2006.

Mansure, A. J., and M. Reiter (1979), A vertical groundwater movement correction for heat flow, *J. Geophys. Res.*, *84*, 3490–3496, doi:10.1029/JB084iB07p03490.

Mareschal, J. C., and H. Beltrami (1992), Evidences for recent warming from perturbed geothermal gradients: Examples from eastern Canada, *Clim. Dyn.*, *6*, 135–143, doi:10.1007/BF00193525.

Menberg, K., P. Blum, B. L. Kurylyk, and P. Bayer (2014), Observed groundwater temperature response to recent climate change, *Hydrol. Earth Syst. Sci.*, *18*, 4453–4466, doi:10.5194/hess-18-4453-2014.

Scanlon, B. R., and P. G. Cooke (2002), Theme issue on groundwater rescharge, *Hydrogeol. J.*, *10*, 3–4, doi:10.1007/s10040-001-0175-3.

Scanlon, B. R., K. E. Keese, A. L. Flint, L. E. Flint, C. B. Gaye, W. M. Edmunds, and I. Simmers (2006), Global synthesis of groundwater recharge in semiarid and arid regions, *Hydrol. Processes*, *20*, 3335–3370, doi:10.1002/hyp.6335.

Swanson, T. E., and M. B. Cardenas (2011), Ex-Stream: A MATLAB program for calculating fluid flux through sediment-water interfaces based on steady and transient temeprature profiles, *Comput. Geosci.*, *37*, 1664–1669, doi:10.1016/j.cageo.2010.12.001.

Taniguchi, M., D. R. Williamson, and A. J. Peck (1999a), Disturbances of temperature-depth profiles due to surface climate change and subsurface water flow: 2. An effect of step increase in surface temperature caused by forest clearing in southwest western Australia, *Water Resour. Res.*, *35*, 1519–1529, doi:10.1029/1998WR900010.

Taniguchi, M., J. Shimada, T. Tanaka, I. Kayane, Y. Sakura, Y. Shimano, S. Dapaah-Siakwan, and S. Kawashima (1999b), Disturbances of temperature-depth profiles due to surface climate change and subsurface water flow: 1. An effect of linear increase in surface temperature caused by global warming and urbanization in the Tokyo Metropolitan Area, Japan, *Water Resour. Res.*, *35*, 1507–1517, doi:10.1029/1999WR900009.

Uchida, Y., and T. Hayashi (2005), Effects of hydrogeological and climate change on the subsurface thermal regime in the Sendai Plain, *Phys. Earth Planet. Inter.*, *152*, 292–304, doi:10.1016/j.pepi.2005.04.008.

Vandersteen, G., U. Schneidewind, C. Anibas, C. Schmidt, P. Seuntjens, and O. Batelaan (2015), Determining groundwater-surface water exchange from temperature-time series: Combining a local polynomial method with a maximum likelihood estimator, *Water Resour. Res.*, *51*, 922–929, doi:10.1002/2014WR015994.

Voss, C. I., and A. M. Provost (2010), SUTRA: A model for saturated-unsaturated, variable-density ground-water flow with solute or energy transport, *Water Resour. Invest. Rep.*, *02-4231*, 201 pp.

Voytek, E. B., A. Drenkellfuss, F. D. Day-Lewis, R. Healy, J. W. Lane, and D. Werkema (2014), 1DTempPro: Analysing temperature profiles for groundwater/surface-water exchange, *Ground Water*, *54*, 298–302, doi:10.1111/gwat.12051.

Zhang, T. J. (2005), Influence of the seasonal snow cover on the ground thermal regime: An overview, *Rev. Geophys.*, *43*, RG4002, doi:10.1029/2004RG000157.